

Modern Physics Letters A
© World Scientific Publishing Company

Directional detection of Dark Matter

Gabriella Sciolla

*Massachusetts Institute of Technology,
Cambridge, MA 02421, USA
sciolla@mit.edu*

Received (November 2008)

Direct detection of WIMPs is key to understand the origin and composition of Dark Matter. Among the many experimental techniques available, those providing directional information have the potential of yielding an unambiguous observation of WIMPs even in the presence of insidious backgrounds. A measurement of the distribution of arrival direction of WIMPs can also discriminate between Galactic Dark Matter halo models. In this article, I will discuss the motivation for directional detectors and review the experimental techniques used by the various experiments. I will then describe the DMTPC detector in more detail.

Keywords: Dark Matter; WIMPs; directionality; review; TPC; DMTPC

PACS Nos.: include PACS Nos.

1. Introduction

Understanding the nature of Dark Matter (DM) is one of the most fascinating and challenging goals of modern physics. Presently, our knowledge on Dark Matter comes entirely from astronomical and cosmological observations¹. We know that its existence is needed to explain the dynamics of galaxies² and galaxy clusters³, and its distribution can be mapped using gravitational lensing⁴. Recent data from WMAP⁵ indicate that Dark Matter is responsible for 23% of the energy budget of the Universe and 83% of its mass. Unfortunately, very little is known about the identity of Dark Matter and its interactions, because DM particles have never been directly observed in the laboratory. The direct detection of Dark Matter is, therefore, of utmost importance for understanding the dominant matter constituent of our Universe.

The most promising candidates for Dark Matter are axions⁶ and Weakly Interacting Massive Particles (WIMPs). WIMPs are especially compelling in that a calculation of their relic abundance from production during the Big Bang is very close to the measured abundance if the particles are weakly interacting and have mass of the order of a few hundred GeV, which is approximately the weak scale. WIMPs arise in many extensions of the Standard Model of particle physics. In

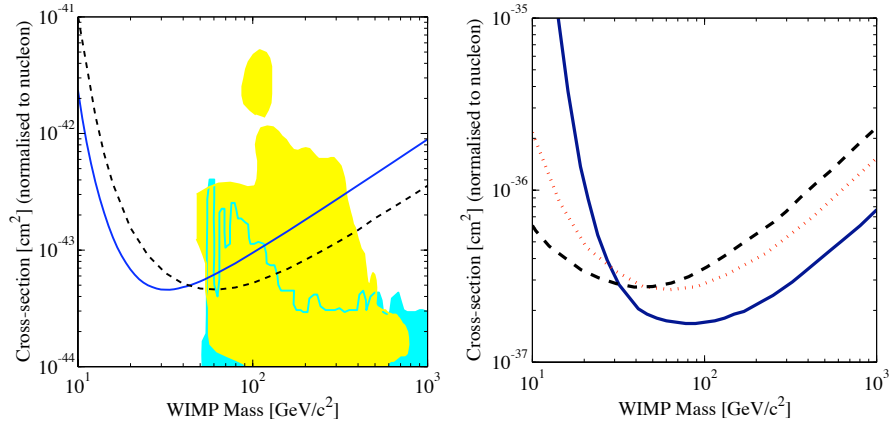
2 *Gabriella Sciolla*


Fig. 1. Recent cross-section limits as a function of the WIMP mass.⁹ Left: limits on spin-independent interactions from CDMS¹⁰ (solid line) and XENON¹¹ (dashed line). The yellow and blue areas show allowed region from theory.^{12,13} Right: limits on spin-dependent interactions on protons from KIMS¹⁴ (solid line), COUPP¹⁵ (dashed line), and NAIAD¹⁶ (dotted line).

Supersymmetric models that conserve R-parity, for example, the Lightest Supersymmetric Particle must be stable, making it a natural candidate for Dark Matter. The favored candidate is the lightest neutralino, which is a mixture of the spin-1/2 partners of the photon, Z^0 , and Higgs particles.

WIMP direct detection experiments look for nuclear recoils due to elastic scattering of DM particles on the nuclei in the active volume of the detector. A WIMP can scatter elastically from a nucleus via two different interactions: spin-independent (SI) and spin-dependent (SD). For spin-independent interactions, the WIMP-nucleus cross-section simply scales with the square of the mass of the nucleus, favoring target materials with high atomic mass. Spin-dependent interactions, in which the spin of the WIMP couples to the spin of the nucleus, require target materials with nonzero spin nuclei⁷ (see Table 2). Spin-dependent cross sections are predicted to dominate over SI cross-sections in models in which the lightest super-symmetric particle has a substantial Higgsino contribution⁸.

Many experiments have been built to detect WIMPs in the laboratory using different experimental techniques. Figure 1 shows the leading experimental limits⁹ on the spin-independent (left) and spin-dependent (right) cross-sections as a function of the WIMP mass. While the limits on SI interactions are already cutting into the theoretically favored region, those on SD interactions, which are presently seven orders of magnitude weaker than the corresponding SI limits, are still two orders of magnitude above the theoretical predictions. A substantial experimental effort is therefore needed to better explore SD interactions.

One of the main challenges in direct detection of Dark Matter is suppression of backgrounds that mimic WIMP-induced nuclear recoils. Today's leading experiments have achieved excellent rejection of the backgrounds that have a distinct

signature in the detector, i.e. photons, electrons and alpha particles. Unfortunately, there are sources of backgrounds for which the detector response is nearly identical to that of a WIMP-induced recoil, such as elastic scattering of neutrons produced either by natural radioactivity or by high-energy cosmic rays. Neutron backgrounds are presently reduced below detection threshold by making use of radio-pure materials in the active area of the experiment, by utilizing active and passive shielding, and by locating the experiments in deep underground caverns. The absence of expected backgrounds simplifies the data analysis, since all observed events are interpreted as signal. However, as the scale of DM experiments grows to fiducial masses of several tons, it will be very hard to completely suppress all neutron backgrounds. In addition, ton-scale experiments will start to detect a new source of irreducible background due to the coherent scattering of solar neutrinos,¹⁸ which no amount of shielding can reduce.

The presence of neutrons and neutrinos will substantially complicate the interpretation of the data, as these insidious backgrounds are not only impossible to reject, but also notoriously difficult to predict.¹⁷ Therefore, when the first hint of a signal of dark matter will be detected, it may be difficult to convince the scientific community about the soundness of the discovery.

A precise knowledge of all backgrounds would not be needed to produce an unambiguous observation of Dark Matter if one could correlate the observation of a nuclear recoil in the detector with some unique astrophysical signature which no background could mimic. This is the idea that motivates directional detection of Dark Matter.

2. The need for directional detection of Dark Matter

The observed rotation curve of our Galaxy suggests that at the galactic radius of the Sun, the galactic potential has a significant contribution from Dark Matter. The Dark Matter distribution in our Galaxy, however, is poorly constrained. A commonly used DM distribution, the standard dark halo model,¹⁹ assumes an isothermal sphere extending up to 50 kpc from the galactic center. The ordinary matter, which forms a disk-like luminous spiral structure at the center, rotates with respect to the halo. Observations show that our solar system orbits around the galactic center on a nearly circular path with an average velocity of about 220 km/s with respect to the DM halo. Therefore, an observer on Earth would see a wind of WIMP particles with average velocity of 220 km/s. In this model, the DM velocity is described by a Maxwell-Boltzman distribution with dispersion $\sigma_v = 155$ km/s.

The Earth's motion relative to the galactic halo leads to an annual modulation²⁰ of the rates of interactions observed above a certain threshold in direct detection experiments. In its seasonal rotation around the Sun, the Earth's velocity has a component that is anti-parallel to the DM wind during the summer, and parallel to it during the winter. Since the velocity of the Earth is about 30 km/s, the apparent velocity of the DM wind will increase (decrease) by about 10% in summer (winter),

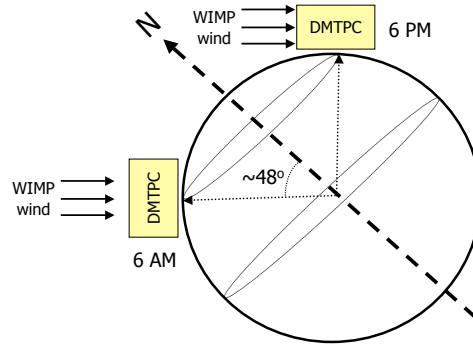


Fig. 2. As the Earth spins about its rotation axis, the average direction of the WIMP wind with respect to a DM detector changes by nearly 90° every 12 sidereal hours.

leading to a corresponding increase (decrease) of the observed rates in DM detectors. Unfortunately, this effect is difficult to detect because the seasonal modulation is expected to be small (a few %) and very hard to disentangle from other systematic effects, such as the seasonal dependence of background rates. These experimental difficulties cast a shadow on the recent claimed observation of the yearly asymmetry by the DAMA/LIBRA collaboration.²¹

A larger modulation of the WIMP signal was pointed out by Spergel²² in 1988 and is illustrated in Figure 2. The Earth spins around its axis with a period of 24 sidereal hours. Because its rotation axis is oriented at 42° with respect to the direction of the DM wind, an observer on Earth sees the average direction of the WIMPs change by nearly 96° every 12 sidereal hours. This modulation in arrival direction should be resolvable by a Dark Matter directional detector, e.g. a detector able to determine the direction of the DM wind. Most importantly, no known background is correlated with the direction of the DM wind. Therefore, a directional Dark Matter detector could hold the key to the unambiguous observation of WIMPs.

In addition to background rejection, the determination of the direction of the arrival of Dark Matter particles can discriminate^{23,24,25} between various DM halo distributions including the standard dark halo model,¹⁹ models with streams of WIMPs, the Sikivie late-infall halo model,²⁶ and other anisotropic models. The discrimination power improves if a determination of the vector direction of WIMPs is possible. This capability makes directional detectors unique observatories for underground WIMP astronomy.

3. Requirements for a directional DM detector

When Dark Matter interacts with normal matter it generates nuclear recoils with typical energies of a few tens of keV (Figure 3-left). The direction of the recoiling nucleus encodes the direction of the incoming DM particle (Figure 3-right). To observe the daily modulation in the direction of the DM wind, an angular resolution of 20–30 degrees in the reconstruction of the recoil nucleus is required.

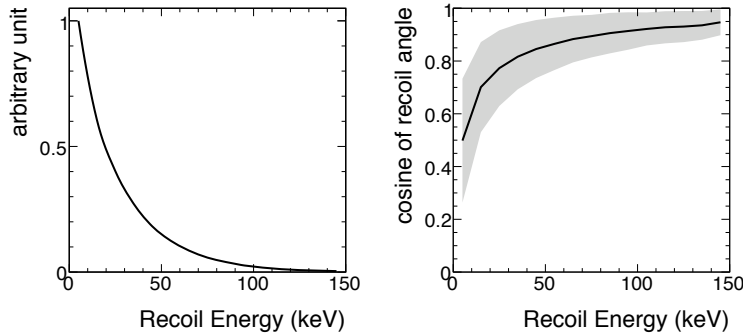


Fig. 3. Energy spectrum (left) and distribution of the cosine of the recoil angle (right) vs. recoil energy for fluorine recoils induced by 100 GeV WIMPs in CF_4 . The recoil angle is defined as the angle between the direction of the recoil and the direction of the incoming particle.

A key requirement for a directional detector is, therefore, to produce nuclear recoil tracks that are at least 1 mm in length, assuming sub-millimeter tracking resolution can be achieved. Long recoils are obtained by using a very dilute gas as a target material. As an example, a typical 50 keV fluorine recoil generated by an elastic collision of a WIMP in CF_4 at 40 torr produces a 2 mm track. The direction of the recoiling nucleus cannot be determined with a conventional DM detector using solid or liquid target because the typical length of a recoil track in such media is less than $1 \mu\text{m}$, well below the tracking resolution of the detector.

An ideal directional detector should provide a 3-D reconstruction of the recoil track with a spatial resolution of a few hundred microns in all three coordinates. A 2-D reconstruction is still valuable, although it degrades the sensitivity.²⁷ It is also very important to be able to determine the sense of the direction by discriminating between the “head” and “tail” of the recoil track. The ability to reconstruct the sense as well as the direction of the recoil improves the sensitivity to DM by about one order of magnitude.²⁷

The advantages associated with directional detectors come at a price: a detector with a fiducial mass of a few tons, necessary to observe DM-induced nuclear recoils, would occupy thousands of cubic meters. It is, therefore, key to the success of the directional DM program to develop detectors with a low cost per unit volume. Since for standard gaseous detectors the largest expense is represented by the cost of the readout electronics, it follows that a low-cost read-out is essential to make DM directional detectors financially viable.

4. Background suppression in directional detectors

The main source of background for any DM experiment is due to electromagnetically interacting particles such as photons, electrons, and alpha particles. These particles are produced by natural radioactivity of the detector components and surrounding materials, as well as by cosmic rays. Most DM experiments can effectively

suppress such backgrounds by using only radio-pure materials in the fabrication of the apparatus, by constructing shielding around the detector, and by rejecting background events in the off-line analysis based on their characteristic signature.

Directional detectors provide an additional signature that can be used to distinguish particle species: the correlation between the energy and length of the recoil track. As an example, in the case of CF_4 gas at a pressure of 50 torr, simulations show that a typical 30 keV fluorine recoil travels about 1 mm. A 15 keV electron, which produces the same net ionization, travels about 30 mm and can be easily distinguished from the signal. A 7 keV α particle has a range of about 1 mm. However, since this energy is much smaller than that of a fluorine ion with the same range, such a low energy α particle can be distinguished from a recoiling nucleus.

Neutrons constitute another source of background. While much less abundant than α particles, photons, or electrons, neutrons are more insidious for DM searches because their signature is indistinguishable from that of a WIMP. Neutrons arise from two independent processes: natural radioactivity (fission and (α, n) reactions), and interactions of high-energy muons in the rock surrounding the detector. The incidence of the former category, which is characterized by a low-energy spectrum of less than 10 MeV,¹⁷ can be effectively reduced with passive shielding (e.g. water or polyethylene). Muon-induced neutrons have a much harder spectrum, with a substantial tail above 10 MeV¹⁷ which reduces the effectiveness of shielding. As a consequence, it is necessary to locate DM detectors in a deep-underground laboratory. In addition, a neutron veto can be used to improve the rejection of such backgrounds.

Directional detectors have an additional advantage with respect to traditional DM detectors in distinguishing neutron backgrounds from WIMP signals: while the signal is expected to be correlated with the direction of the WIMP wind, recoils from neutrons are either isotropically distributed, or point back to some particular regions in the detector where radioactive material is present.

Finally, directionality is key to distinguish between coherent scattering from solar neutrinos from WIMP signal: while neutrinos will point back to the Sun, the signal will follow the direction of the DM wind.

5. Existing directional detectors

The properties of the current directional Dark Matter experiments are summarized in Table 1. Most directional detectors are Time Projection Chambers²⁸ (TPCs) that use the gas both as target and detector material. The pressure of the gas inside the vessel is chosen in the range 40-100 torr. At this pressure a typical collision of a 100 GeV WIMP of 220 km/s with a gas molecule causes a nucleus to recoil about 1-2 mm. The ionization electrons produced by the recoiling nucleus drift in the gas along a uniform electric field toward an anode plane. The intense electric field around the anodes triggers an avalanche that amplifies the signal which allows us to reconstruct the projection of the 3-D nuclear recoil on the 2-D anode plane.

Table 1. Summary of existing directional Dark Matter experiments.

Experiment	Gas	Interactions	Technology	Readout
DRIFT	CS ₂	SI	Negative ion TPC	MWPC
NewAge	CF ₄	SD/SI	TPC	μ PIC
MIMAC	³ He/CF ₄	SD/SI	TPC	Electronic 2-D
DMTPC	CF ₄	SD/SI	TPC	Optical 2-D

The time between the beginning and the end of the signal determines the length of the nuclear recoil in the direction parallel to the drift. Because the energy loss (dE/dx) is not uniform along the trajectory, the sense of the recoiling nucleus can be determined (“head-tail” measurement).

The field of Dark Matter directional detection was pioneered by the DRIFT²⁹ experiment, which uses a negative ion time projection chamber³⁰ filled with carbon-disulfate (CS₂) gas at a pressure of 40 torr. Drifting negative ions instead of electrons reduces diffusion, thereby allowing for drift distances of up to 50 cm without significant loss in spatial resolution and without the need for a magnetic field. The detector is read out by multi-wire proportional counters (MWPCs).

A full-size DRIFT module³¹ is currently taking data at the Boulby Underground Laboratory at a depth of 2,805 meters water equivalent. The fiducial volume of this detector is $1 \times 1 \times 1 \text{ m}^3$, corresponding to 167 g of CS₂. The apparatus consists of a 1.5 m³ low-background stainless steel vacuum vessel containing two back-to-back TPCs with a shared, vertical, central cathode constructed of 20 μm stainless steel wires. Two field cages, located on either side of the central cathode, define two 50 cm long drift regions. Charge readout of tracks was provided by two MWPCs each comprised of an anode plane of 20 μm stainless steel wires sandwiched between two perpendicular grid planes of 100 μm stainless steel wires. The detector is operated at a gas gain of 10^3 , and the drift electric field is 624 V/cm. Both cathode and anode wires are multiplexed and reduced to 8 channels of readout per wire plane. Because the pitch of the wires in the MWPC is 2 mm, the eight adjacent readout lines (either grid or anode) sample a distance of 16 mm, which is sufficient to fully contain a WIMP candidate.

The gas gain of the detector is monitored every 6 hours with a precision of 2% by using a retractable ⁵⁵Fe calibration source. The gamma-ray rejection capability of the detector, determined using ⁶⁰Co sources, is better than 8×10^{-6} . A ²⁵²Cf source is used to demonstrate an efficiency of 94% in detecting nuclear recoils of sulfur (carbon) above a threshold of 47 (31) keV. The efficiency decreases to 60% after off-line WIMP selection criteria are applied.

While analyzing the 10.2 kg days of data collected underground with a shielded DRIFT detector, an unexpected population of nuclear recoil events has been observed, and shown to be due to the decay of the daughter nuclei of ²²²Rn which have attached to the central cathode. Reduction of the radon inside the detector components, as well as development of additional measures to remove or veto Rn

8 *Gabriella Sciolla*

events, is underway.

Laboratory runs using ^{252}Cf sources demonstrate that DRIFT can measure the range of the recoil tracks in 3-D with adequate precision,³² and show statistical discrimination in determining the sense of the recoil down to a threshold of 50 keV.³³ To improve the 3-D reconstruction capability of the detector, the possibility of using Micromegas³⁴ detectors as an alternative form of readout³⁵ is being investigated.

The NewAge^{36,37} experiment uses CF_4 gas to detect spin-dependent interactions of WIMPs. The apparatus is a time projection chamber with a micro pixel (μ -PIC) readout. A μ -PIC is a two-dimensional position-sensitive detector manufactured with printed circuit board technology, and provides gas multiplication and readout. Additional gas amplification³⁸ is provided by a gas electron multiplier (GEM), for a total gas gain of 5×10^4 .

A NewAge detector with a fiducial volume of $23 \times 28 \times 30 \text{ cm}^3$ is currently taking data in the Kamioka mine. The detector is contained in a stainless-steel vacuum chamber and operates at a pressure between 30 and 150 torr. The drift length is limited to 30 cm by transverse diffusion. The uniformity of the electric field in the drift region is maintained by a field-shaping pattern on a fluorocarbon circuit board surrounding the detection volume. An α source is used to calibrate and monitor the gain of the detector. The energy resolution is measured to be better than 70% in the range relevant to DM studies, while the spatial resolution is 800 μm . The efficiency of the detection of nuclear recoils is measured to be 40% at 100 keV using a ^{252}Cf source. The gamma ray rejection factor is measured using ^{137}Cs to be 6×10^{-4} .

Spin-dependent interactions are also pursued by the MIMAC³⁹ collaboration. MIMAC is a micro-TPC with an avalanche amplification with a pixelized anode. The target materials are ^3He and CF_4 . The use of ^3He is motivated by its light mass, which makes it more sensitive to low mass WIMPs. In addition, ^3He has unique properties in terms of gamma ray rejection power and discrimination against neutron backgrounds.³⁹ MIMAC plans to run at two pressures: high pressure (1-3 bar) in the initial phase of the experiment, and low pressure (100-200 mbar) after DM candidates will be observed and directional information will be needed to discriminate against backgrounds.

Finally, a group from Nagoya University has proposed⁴⁰ to use emulsions to image the nuclear recoils caused by WIMP interactions. Emulsions, with their sub-micron 3-D spatial resolution, can determine the direction of WIMPs even from very short recoils. The target density can, therefore, be much higher than in gaseous directional detectors, and a large fiducial mass can be contained in a relatively small volume. The limitation of this detector has to do with the fact that long integration time may smear the directional signal. In addition, an efficient rejection of backgrounds such as very low energy α particles and electrons may be more challenging to achieve than in other directional detectors.

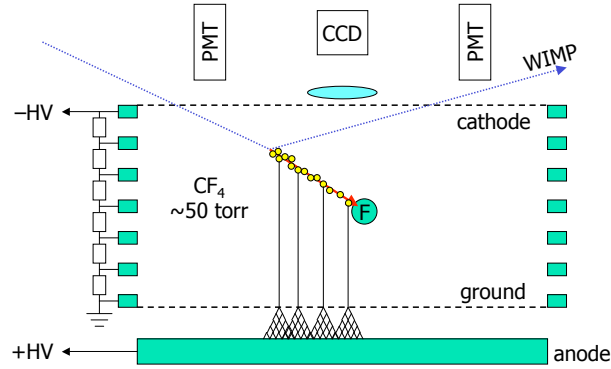


Fig. 4. Illustration of the DMTPC detector concept.

6. The DMTPC detector

The DMTPC detector is a low-pressure TPC with optical readout. The detection principle is illustrated in Figure 4. The TPC is filled with tetrafluoromethane (CF_4) at a pressure of about 50 torr. At this pressure, a typical 50 keV nuclear recoil has a length of about 2 mm. The electrons liberated by the recoiling nuclei drift toward the amplification region, where photons are produced together with electrons in the avalanche process. A CCD camera mounted above the cathode mesh images these photons recording the projection of the 3-D nuclear recoil on the 2-D amplification plane. An array of photomultipliers (PMTs) mounted above the cathode mesh measures the length of the recoil in the drift direction.

6.1. CF_4 gas

CF_4 was chosen as target material primarily because of its high content in fluorine. Fluorine is an excellent element⁴¹ to detect spin-dependent interactions on protons, due to its large spin factor and isotopic abundance, as shown in Table 2.

In addition, CF_4 is an excellent detector material^{42,43}. Its good scintillation properties are very important because of the optical readout. Recent measurements⁴⁴ indicates that in CF_4 the number of photons produced between 200 and 800 nm is about 1 for every 3 avalanche electron. Moreover, the low transverse diffusion characteristic of CF_4 allows for a good spatial resolution in the reconstruction of the recoil track despite the long (25 cm) drift distance. Finally, CF_4 is non-flammable and non-toxic, and, therefore, safe to operate underground.

6.2. Amplification region

Two alternative implementations of the amplification region⁴⁵ are illustrated in Figure 5. In the first design (Figure 5-left), the amplification is obtained by applying a large potential difference ($\Delta V = 0.6\text{--}1.1$ kV) between a copper plate and a conductive woven mesh. A uniform distance of 540 μm between the plate and the mesh

Table 2. Spin of the nucleus (J), nuclear spin factor ($\lambda^2 J(J+1)$) and abundance in nature of various isotopes considered for SD-interaction measurements. The figure of merit, to be used to compare the various isotopes, is defined as the product of the square of the nucleus mass, the number of isotopes per kg, and the spin factor.

Isotope	J	$\lambda^2 J(J+1)$	Natural abundance	Figure of merit
^1H	1/2	0.75	100%	5
^{19}F	1/2	0.65	100%	74
^{23}Na	3/2	0.04	100%	6
^{73}Ge	9/2	0.06	7.8%	2
^{93}Nb	9/2	0.16	100%	91
^{127}I	5/2	0.01	100%	5
^{129}Xe	1/2	0.12	26%	25

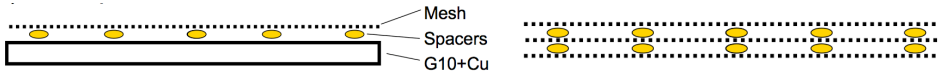


Fig. 5. Two designs for the DMTPC amplification region: the “mesh-plate” design is shown on the left, and the triple mesh design is shown on the right.

is ensured by the use of fishing wires spaced 2 cm apart. The copper or stainless steel mesh is made of 28 μm wire with a pitch of 256 μm . The pitch of the mesh determines the intrinsic spatial resolution of the detector.

In a second design (Figure 5-right), the copper plate is replaced with two additional woven meshes. This design has the advantage of creating a transparent amplification region, which enables a single CCD camera to image two drift regions. This allows for a substantial cost reduction.

6.3. Optical readout

Optical readouts for directional DM experiments were first explored in the 1990s⁴⁶. CCDs provide a true 2-D readout at a much lower cost per channel than any other technology used in particle physics. A modern low-noise CCD camera with 4 megapixels can be purchased today for a few thousand US dollars, which corresponds to 10^{-3} dollars/channel. Because the cost of the readout electronics dominates the overall cost of a directional DM detector, the choice of an optical readout makes directional detectors economically viable. Widespread use of CCD cameras from cell phones to medical x-ray drives the development of new and more efficient CCDs. As a result, better products are available every year at decreasing prices.

A detector with an optical readout needs a well-designed optics. Because the average ionization energy in CF_4 is 54 eV,³⁷ a typical nuclear recoil with an energy of 50 keV will produce about 10^3 primary electrons. Typical gas gains in the amplification region are of the order of 10^5 , and the ratio of photons to electrons produced in the amplification is 1:3. Therefore, the number of photons produced in

the amplification region is about 10^7 . The fraction of the photons that are collected by the lens and detected by the CCD depends on the solid angle covered by the lens. As an example, for a lens aperture of 25 mm and a distance of 30 cm from the amplification plane, the number of photons detected is 10^2 – 10^3 , after taking into account the transmittance of the meshes and the lens, and the quantum efficiency of the CCD. Another consideration is the area of the amplification region that can be covered by a single camera. Optics with wide a field of view reduces the number of cameras and, therefore, the cost of the detector. Optimizing the lens design is clearly of crucial importance.

6.4. Measurement strategy

The DMTPC detector is designed to measure the following quantities:

- (i) the number of photons observed in the CCD camera;
- (ii) the 2-D image of the recoiling nucleus;
- (iii) the distribution of energy loss along the recoil track;
- (iv) the width and integral of the PMT signal;
- (v) the electronic signal produced on the amplification plane.

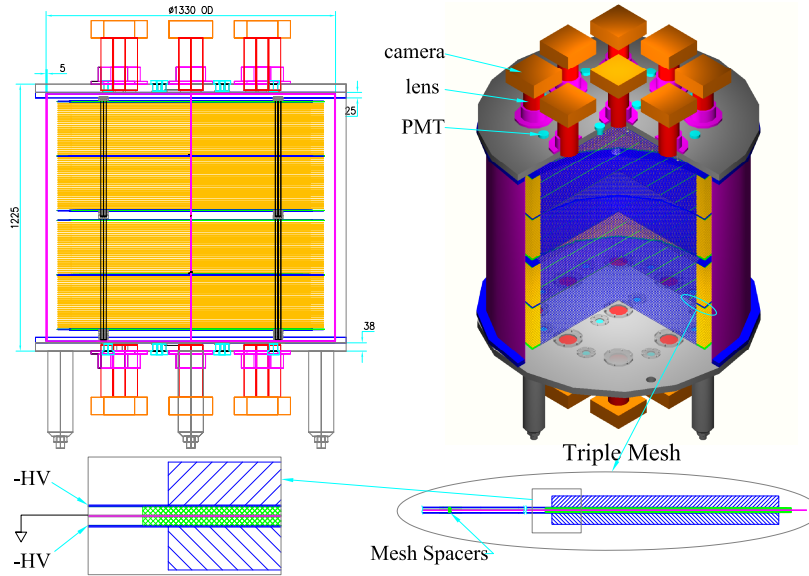
The energy of the nuclear recoil is independently determined by the measurement of the number of photons observed in the CCDs, the integral of the electronic signal produced on the amplification mesh, and the integral of the PMT signal. The redundancy in the design is intentional and has the goal of maximizing the robustness of the measurement. The track length and direction of the recoiling nucleus is reconstructed by combining the measurement of the projection along the amplification plane (from pattern recognition in the CCD) and the projection along the direction of drift, determined from the width of the signal recorded in the PMTs. The sense of the recoil track can be determined by the Bragg curve, the characteristic variation of the energy deposit along the length of the track.

The CCD images have a long (about 1 second) exposure. If during the exposure a trigger is generated by the PMT or the electronic read out of the amplification plane, the CCD is read out and the event is saved to disk. Otherwise, the CCD is reset, to minimize dead time.

The combination of the measurements described above is very effective in reconstructing the energy, direction, and sense of nuclear recoils from WIMPs. In addition, an excellent rejection of the electromagnetic backgrounds can be obtained by combining the measurement of the energy and length of the recoil. The gamma ray rejection factor, measured using a ^{137}Cs source, is better than 2 parts per million.

6.5. Detector design

The preliminary design of a 1-m^3 DMTPC detector is shown in Figure 6. The apparatus consists of a stainless steel vessel of 1.3 m diameter and 1.2 m height.

12 *Gabriella Sciolla*

 Fig. 6. Preliminary drawings of the 1 m^3 DMTPC detector.

Nine CCD cameras and nine PMTs are mounted on each of the top and bottom plates of the vessel, separated from the active volume of the detector by an acrylic window. The detector consists of two optically separated regions. Each of these regions is equipped with a triple-mesh amplification device, mounted in between two symmetric drift regions. Each drift region has a diameter of 1.2 m and a height of 25 cm, for a total active volume of 1 m^3 . A field cage made of stainless steel rings keeps the uniformity of the electric field within 1% in the fiducial volume. A gas system recirculates and purifies the CF_4 .

All materials used inside the active volume of the detectors are required to be radio-pure to limit backgrounds from internal radioactivity. Pure copper, stainless steel, and acrylic are known to satisfy these requirements.⁴⁷ Because all CCD cameras and lenses are outside the active volume, their contribution to internal radioactivity is minimal.

When operating the detector at a pressure of 50 torr and 21 degrees C, this module will contain 250 g of CF_4 . Assuming an overall data-taking efficiency of 50%, a one-year underground run will yield an exposure of 45 kg-days.

6.6. *R&D results*

The current DMTPC prototype consists of two optically independent regions contained in one stainless steel vessel. Each region is a cylinder with 25 cm diameter and 25 cm height contained inside a field cage. The amplification is obtained by using a mesh-plate design. The detector is read out by two CCD cameras, each imaging one

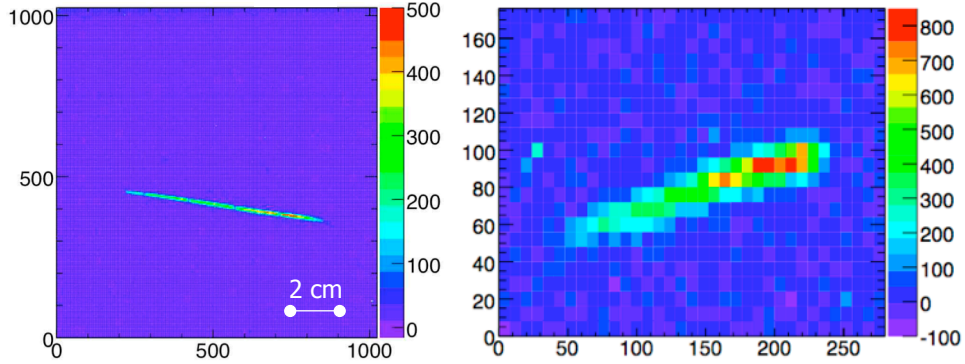


Fig. 7. Left: an α track stopped in CF_4 at a pressure of 100 torr. The particle travels left to right. The red region on the right of the track corresponds to the Bragg peak. Right: a nuclear recoil from a low-energy neutron in CF_4 at 75 torr. The neutron, produced by a ^{252}Cf source, was traveling right to left. The higher dE/dx visible on the right of the track is consistent with observation of the “head-tail” effect.

drift region. The optical system uses two Nikon photographic lenses with f-number of 1.2 and focal length of 55 mm, and two Apogee U6 CCD cameras⁴⁸ equipped with Kodak 1001E CCD chips. Because the total area imaged is $16 \times 16 \text{ cm}^2$, the detector has an active volume of about 10 liters.

The main calibration source is a ^{241}Am source that produces 5.5 MeV alpha particles. The image of one alpha particle stopped inside CF_4 at 100 torr is shown in Figure 7(left). This source is used to study the gain of the detector as a function of the voltage in the amplification region and gas pressure, while a ^{55}Fe is used for absolute energy calibration. The alpha source is also used to measure the resolution as a function of the drift distance of the primary electrons to quantify the effect of the diffusion. These studies⁴⁹ show that the transverse diffusion is $\approx 1 \text{ mm}$ for a drift distance of 25 cm.

The performance of the DMTPC detector in determining the sense and direction of nuclear recoils has been evaluated by studying the recoil of fluorine nuclei in interaction with low-energy neutrons. When the nuclear recoil produced is below 1 MeV, the energy deposition decreases along the path of the recoil, allowing for the identification of the “head” (“tail”) of the event by a smaller (larger) energy deposition. To quantify this effect, we define the skewness $s \equiv \langle x^3 - \langle x \rangle^3 \rangle / \langle x^2 - \langle x \rangle^2 \rangle^{3/2}$ where x is the position along the recoil track, signed according to the direction of the neutron beam, and the angle brackets denote averages weighted by the light yield. Decreasing light yield along the recoil track should result in a negative value of s .

The initial measurements, performed with a wire-based prototype, used 14 MeV neutrons from a deuteron-triton generator. The reconstructed recoils had energy between 200 and 800 keV. The “head-tail” effect was observed with a significance of 8σ .⁴⁹

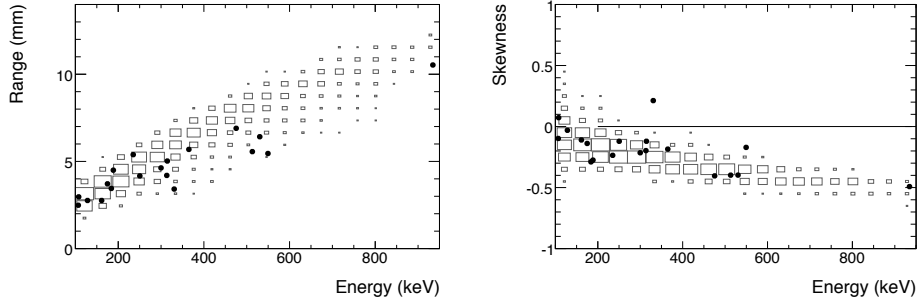


Fig. 8. Range (left) and skewness (right) vs. reconstructed energy for nuclear recoil candidates in a ^{252}Cf exposure at 75 torr. Black points are data, the box-histogram is simulation.

Subsequent measurements used lower energy neutrons generated by a ^{252}Cf source, and a mesh-based detector to obtain a 2-D reconstruction of the nuclear recoils. Better sensitivity to lower energy thresholds was achieved by lowering the CF_4 pressure to 75 torr. Figure 7(right) shows a Cf-induced nuclear recoil reconstructed in the DMTPC detector. The neutron was traveling right to left. The decreasing dE/dx along the track direction clearly visible in the image proves that the detector is able to determine the sense of the direction on an event-by-event basis. Measurements of the length and skewness of the recoil tracks as a function of their energy are shown in Figure 8. The data is in good agreement with the predictions of the SRIM⁵⁰ MC. These measurements establish⁴⁵ good head-tail discrimination for recoils above 100 keV. The “head-tail” discrimination is expected to extend to recoils above 50 keV when the detector is operated at a pressure of 50 torr.

6.7. *Expected sensitivity*

The sensitivity of the DMTPC detector to SD interactions of WIMPs on protons has been studied. In the calculation, it is assumed that the detector will be operated at a threshold of 50 keV in an underground laboratory at a depth of 4,300 m.w.e. and that it will be surrounded by a neutron shielding consisting of 40 cm of polyethylene. No significant internal backgrounds are assumed to be present above threshold.

The limits expected for exposures of 0.1 and 100 kg-years are shown in Figure 9. The dashed lines in the same figure show the present best limit on spin-dependent interactions from the KIMS,¹⁴ COUPP,¹⁵ and NAIAD¹⁶ collaborations.

Improvements of a factor of 50 over the best existing measurements can be obtained with 0.1 kg-year exposure, which can be achieved operating a 1-m³ detector for less than one year. The high sensitivity is achieved despite of the limited target mass due to the excellent properties of fluorine for the study of SD interactions (Table 2) and because of the excellent background rejection capability of the detector.

A larger detector, with an active mass of 10^2 – 10^3 kg, will be able to explore a

significant portion of the Minimal Supersymmetric Standard Model (MSSM) parameter space⁵¹. This detector is an ideal candidate for the DUSEL laboratory in South Dakota.

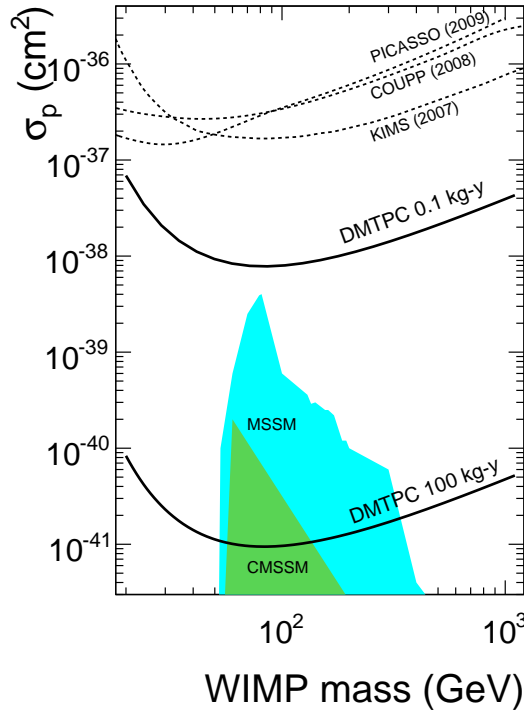


Fig. 9. Expected sensitivity (90% C.L.) to spin-dependent WIMP scattering on protons for a DMTPC detector assuming two different exposures. The dashed lines show the best published limits. The shaded area shows the allowed region from MSSM calculations.

7. Conclusion

Directional detectors can provide an unambiguous positive observation of Dark Matter particles even in presence of insidious backgrounds, such as neutrons or neutrinos. Moreover, the measurement of the direction of the incoming WIMPs will allow us to discriminate between the various DM models in our galaxy, opening the path to underground WIMP astronomy.

In the past few years, several groups have investigated new ideas to develop directional Dark Matter detectors. Low-pressure TPCs are well suited for the purpose, if a 3-D reconstruction of the nuclear recoil can be achieved using an inexpensive readout, and an effective rejection of electromagnetic backgrounds can be obtained.

The DMTPC experiment addresses both of these requirements. This detector measures the energy, direction, and sense of the nuclear recoils produced in elastic collisions of WIMPs in low-energy CF_4 gas. The redundancy between the various measurements allows for excellent background rejection, while the use of an optical readout substantially reduces the costs, which makes a ton-size directional detector economically viable. The choice of CF_4 as the target material makes this detector particularly suited to study SD interactions, complementing the effort of most other DM experiments (e.g. noble liquid detectors), more suitable for the study of SI interactions.

Acknowledgments

I am grateful to my DMTPC collaborators and, in particular, to D. Dujmic, H. Wellenstein, and A. Lee for contributing some of the plots and results used in this paper. In addition, I wish to thank M. Morii and J. Battat for useful discussions and for proofreading the manuscript. This work is supported by the U.S. Department of Energy (contract number DE-FG02-05ER41360) and the MIT Physics Department.

References

1. V. Trimble, *Ann. Rev. Astron. Astrophys.* **25**, 425 (1987).
2. V. C. Rubin, N. Thonnard and W. K. Ford, *Astrophys. J.* **238**, 471 (1980).
3. F. Zwicky, *Helv. Phys. Acta* **6**, 110 (1933).
4. N. Kaiser and G. Squires, *Astrophys. J.* **404**, 441 (1993).
5. G. Hinshaw *et al.* [WMAP Collaboration], *Astrophys. J. Suppl.* **180**, 225 (2009).
6. R. D. Peccei and H. R. Quinn, *Phys. Rev. D* **16**, 1791 (1977); R. D. Peccei and H. R. Quinn, *Phys. Rev. Lett.* **38**, 1440 (1977); S. Weinberg, *Phys. Rev. Lett.* **40**, 223 (1978); F. Wilczek, *Phys. Rev. Lett.* **40**, 279 (1978); J. Preskill, M. B. Wise and F. Wilczek, *Phys. Lett. B* **120**, 127 (1983); L. F. Abbott and P. Sikivie, *Phys. Lett. B* **120**, 133 (1983); M. Dine and W. Fischler, *Phys. Lett. B* **120**, 137 (1983).
7. G. Jungman, M. Kamionkowski and K. Griest, *Phys. Rept.* **267**, 195 (1996).
8. U. Chattopadhyay and D. P. Roy, *Phys. Rev. D* **68**, 033010 (2003); B. Murakami and J. D. Wells, *Phys. Rev. D* **64** (2001) 15001; J. Vergados, *J. Phys. G* **30** (2004) 1127; J. R. Ellis, A. Ferstl and K. A. Olive, *Phys. Rev. D* **63**, 065016 (2001); J. R. Ellis, A. Ferstl and K. A. Olive, *Phys. Lett. B* **481** 304 (2000); G. Bertone, D. G. Cerdeno, J. I. Collar and B. C. Odom, *Phys. Rev. Lett.* **99**, 151301 (2007).
9. Plots were obtained using <http://dmtools.berkeley.edu/limitplots/>.
10. Z. Ahmed *et al.* [CDMS Collaboration], *Phys. Rev. Lett.* **102**, 011301 (2009).
11. J. Angle *et al.* [XENON Collaboration], *Phys. Rev. Lett.* **100**, 021303 (2008).
12. E. A. Baltz and P. Gondolo, *JHEP* **0410**, 052 (2004).
13. L. Roszkowski, R. Ruiz de Austri and R. Trotta, *JHEP* **0707**, 075 (2007).
14. H. S. Lee. *et al.* [KIMS Collaboration], *Phys. Rev. Lett.* **99**, 091301 (2007).
15. E. Behnke *et al.* [COUPP Collaboration], *Science* **319**, 933 (2008).
16. G. J. Alner *et al.* [UK Dark Matter Collaboration], *Phys. Lett. B* **616**, 17 (2005).
17. D. Mei and A. Hime, *Phys. Rev. D* **73**, 053004 (2006).
18. J. Monroe and P. Fisher, *Phys. Rev. D* **76**, 033007 (2007).
19. J. N. Bahcall and R. M. Soneira, *Astrophys. J. Suppl.* **44**, 73 (1980); J. A. R. Caldwell

- and J. P. Ostriker, *Astrophys. J.* **251**, 61 (1981); M. S. Turner, *Phys. Rev. D* **33**, 889 (1986); R. A. Flores, *Phys. Lett. B* **215**, 73 (1988).
20. A. K. Drukier, K. Freese, and D. N. Spergel, *Phys. Rev. D* **33**, 3495 (1986); K. Freese, J. A. Frieman and A. Gould, *Phys. Rev. D* **37**, 3388 (1988).
 21. R. Bernabei *et al.* [DAMA Collaboration], *Eur. Phys. J. C* **56**, 333 (2008).
 22. D. N. Spergel, *Phys. Rev. D* **37**, 1353, (1988).
 23. M. S. Alenazi and P. Gondolo, *Phys. Rev. D* **77**, 043532 (2008).
 24. B. Morgan, A. M. Green and N. J. C. Spooner, *Phys. Rev. D* **71**, 103507 (2005).
 25. C. J. Copi, J. Heo and L. M. Krauss, *Phys. Lett. B* **461**, 43 (1999); C. J. Copi and L. M. Krauss, *Phys. Rev. D* **63**, 043507 (2001).
 26. P. Sikivie, I. I. Tkachev and Y. Wang, *Phys. Rev. Lett.* **75**, 2911 (1995); P. Sikivie, I. I. Tkachev and Y. Wang, *Phys. Rev. D* **56**, 1863 (1997); P. Sikivie, *Phys. Rev. D* **60**, 063501 (1999); F. S. Ling, P. Sikivie and S. Wick, *Phys. Rev. D* **70**, 123503 (2004).
 27. A. Green and B. Morgan, *Astropart. Phys.* **27**, 142 (2007).
 28. D. Nygren, *In "Stanford 1976, PEP Conference", Stanford 1976, O1-06*; D. Fancker *et al.*, *Nucl. Instrum. Meth.* **161**, 383 (1979).
 29. G. J. Alner *et al.*, *Nucl. Instrum. Meth. A* **555**, 173 (2005).
 30. C. J. Martoff *et al.*, *Nucl. Instrum. Meth. A* **440**, 355 (2000).
 31. S. Burgos *et al.*, *Astropart. Phys.* **28**, 409 (2007).
 32. S. Burgos *et al.*, *Nucl. Instrum. Meth. A* **600**, 417 (2009).
 33. S. Burgos *et al.*, arXiv:0809.1831 [astro-ph].
 34. Y. Giomataris *et al.*, *Nucl. Instrum. Meth. A* **376**, 29 (1996).
 35. P. K. Lightfoot *et al.*, *Astropart. Phys.* **27**, 490 (2007).
 36. K. Miuchi *et al.*, *Phys. Lett. B* **654**, 58 (2007).
 37. T. Tanimori *et al.*, *Phys. Lett. B* **578**, 241 (2004).
 38. K. Miuchi *et al.*, *Nucl. Instrum. Meth. A* **576**, 43 (2007).
 39. D. Santos *et al.*, *J. Phys. Conf. Ser.* **65**, 012012 (2007).
 40. T. Naka *et al.*, *Nucl. Instrum. Meth. A* **581**, 761 (2007).
 41. J. Ellis and R. A. Flores, *Phys. Lett. B* **263**, 259 (1991).
 42. A. Pansky *et al.*, *Nucl. Instrum. Meth. A* **354**, 262 (1995).
 43. L. G. Christophorou, *et. al.*, *J. Phys. Chem. Ref. Data* **25**, 1341 (1996)
 44. A. Kaboth *et al.*, [DMTPC Collaboration], *Nucl. Instrum. Meth. A* **592**, 63 (2008).
 45. D. Dujmic *et al.*, [DMTPC Collaboration], *Astropart. Phys.* **30**, 58 (2008).
 46. K. N. Buckland *et al.*, *Phys. Rev. Lett.* **73**, 1067 (1994).
 47. D. S. Leonard *et al.*, *Nucl. Instrum. Meth. A* **591**, 490 (2008).
 48. See Apogee web site: www.ccd.com.
 49. D. Dujmic *et al.*, [DMTPC Collaboration], *Nucl. Instrum. Meth. A* **584** 327 (2008).
 50. J. F. Ziegler *et al.*, Pergamon Press, New York, 1985.
 51. J. R. Ellis, A. Ferstl and K. A. Olive, *Phys. Rev. D* **63**, 065016 (2001); J. R. Ellis, A. Ferstl and K. A. Olive, *Phys. Lett. B* **481** 304 (2000).